ACS APPLIED MATERIALS & INTERFACES

Research Article

www.acsami.org

High-Accuracy Analysis of Nanoscale Semiconductor Layers Using Beam-Exit Ar-Ion Polishing and Scanning Probe Microscopy

Alexander J. Robson,*[,†] Ilya Grishin,[†] Robert J. Young,[†] Ana M. Sanchez,[‡] Oleg V. Kolosov,[†] and Manus Hayne[†]

[†]Department of Physics, Lancaster University, Lancaster, LA1 4YB, United Kingdom

[‡]Department of Physics, University of Warwick, Coventry, CV4 7AL, United Kingdom

ABSTRACT: A novel method of sample cross sectioning, beam-exit Ar-ion cross-sectional polishing, has been combined with scanning probe microscopy to study thin $Al_xGa_{1-x}As$/GaAs layers. Additional contrast enhancement via a citric acid/hydrogen peroxide etch allows us to report the observation of layers as thin as 1 nm. Layer thickness measurements agree with transmission electron microscopy (TEM) data to 0.1 ± 0.2 nm, making this a very promising low-cost method for nanoscale analysis of semiconductor heterostructures.

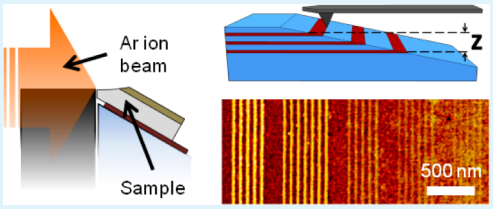

KEYWORDS: *scanning probe microscopy, cross-sectional analysis, semiconductor nanostructure layers, transmission electron microscopy, nanoscale metrology, selective etching*

INTRODUCTION

Semiconductor nanostructure devices are complex structures which rely on precise dimensions; small variations can cause extensive changes to device properties. It is often essential to obtain a cross-sectional analysis of the sample, if only to determine whether the actual device matches the design. For III−V semiconductor samples, much of this work is carried out using transmission electron microscopy (TEM). This method requires careful sample preparation; combined with only a limited number of available facilities it is inevitably an expensive process. As such, investigating other methods to identify buried nanostructures is advantageous. Scanning probe microscopy (SPM), with its nanometer-scale precision and unique sensitivity to surface material properties through a wide range of techniques, is a common tool available in most facilities. Combined with cross-sectioning, SPM is a promising candidate for identifying and analyzing subsurface structures. Here we report the use of a novel cross-sectioning method, beam-exit Ar-ion cross-sectional polishing (BEXP),[1,2] in combination with selective etching and SPM to measure thicknesses of nanoscale semiconductor layers with an accuracy that approaches that of TEM.

Various methods exist for cross-sectioning samples. Mechanical grinding and polishing,[3] a low cost technique, is generally unsuitable for SPM as it can result in sample damage and contamination by abrasive particles. Ion-beam polishing methods, such as focused ion beam (FIB) and Ar ion polishing, are therefore better suited for SPM studies. However, although FIB is an established technique for preparing TEM samples,[4] the limited beam size means that this is a slow method for producing the macroscopic-scale sections required for SPM, which relies on optical methods to determine the area of interest. Furthermore, the ion bombardment in FIB also generates peripheral damage to the sample, which can increase the amount of TEM and SPM characterization artifacts.

Ar-ion beam milling, a related technique, is also used for sample thinning for TEM[5] as well as cross-sectional polishing for scanning electron microscopy samples.[6,7] Cross sections are produced by mounting the sample next to a masking plate. A broad Ar-ion beam is directed normally to the sample surface, rapidly milling the unshielded section of the sample (Figure 1a). Although the majority of the cut has roughness on the nanoscale, the first few micrometers of the cut at the beam-entry point have a high degree of curvature and low surface quality, rendering them unsuitable for characterization of nanoscale structures. As most semiconductor device structures are grown on top of a large substrate, and thus tend to be in the top few hundreds to thousands of nanometers of the sample, regular Ar-ion beam cross sectioning is, in general, unsuitable for studying semiconductor devices.

A recently developed method, BEXP,[1,2] modifies this configuration. The sample position is rotated, so that rather than entering through the top, the ion beam impinges upon the side of the sample at a shallow angle and exits the surface far from the masking plate (Figure 1(b). This beam-exit point exhibits a much lower (true nanometer-scale) surface roughness than the area close to the mask, making it suitable for SPM. As BEXP cuts at an angle, the layers within the sample are "stretched out" over a larger area when compared to a traditional cross section, allowing easier determination of small structures. Also, such geometry produces an in-depth section that is only slightly tilted with respect to the sample surface, so both can be imaged in one SPM scan. This close-to-flat surface

Received: January 21, 2013
Accepted: March 25, 2013
Published: March 25, 2013

   dx.doi.org/10.1021/am400270w | *ACS Appl. Mater. Interfaces* 2013, 5, 3241−3245

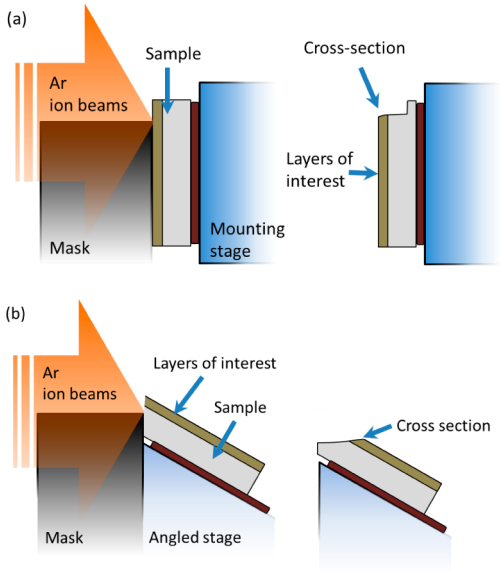

Figure 1. (a) Conventional Ar-ion beam cutting. The layers of interest lie close to the beam entry point. This area of the cut is strongly affected by the proximity of the mask, making SPM imaging of near-surface structures impossible. (b) Beam-exit Ar-ion cross-sectional polishing. The area of interest is far from the mask and only exposed to the beam-exit. Roughness here is of nanometer-scale values, making it suitable for SPM imaging of near surface structures.

is very favorable for high-performance SPM imaging, and the presence of top and cross sectioned areas in the image facilitates the identification of the area and the morphology of the subsurface nanostructures. Specifically, this setup is achieved by first attaching the sample to a premanufactured angled holder (usually 5−30°) with a temporary adhesive, in this case wax with a low melting-point. In order to keep the ion beam perpendicular to the surface at the entry point, the geometry of the sample is modified using a mechanical lapping and polishing technique with several grades of diamond paper. Great care must be taken at this stage as irregularities present in the surface may affect the quality of the cut. The preangled holder and sample are then placed within a Leica EM TIC020 triple ion-beam cutter, which uses three Ar-ion beams mounted in a plane to form a wide milling-region sector of 100°.[8] The sample is positioned 20−40 μm above the masking plate, resulting in a cut approximately 2−3 mm wide and 200 μm deep (dependent on the mounting angle and entry point). The Leica system allows Ar-ion accelerating voltage within a 1−8 kV range. Cuts are initially milled at 5−7 kV until the process reaches the area of interest (usually 2−3 h). The voltage is then reduced to 1 kV to polish the surface at a lower energy for 15−30 min.

For this study, we have used a series of $Al_xGa_{1-x}As$/GaAs superlattices with varying layer thickness and composition grown via molecular beam epitaxy. Contrast was initially provided by allowing samples to oxidize before scanning. $Al_xGa_{1-x}As$ rapidly oxidizes in ambient conditions, with oxidized $Al_xGa_{1-x}As$ layers protruding out from the surrounding GaAs, with a height that is dependent on Al content x.[9] Although this oxidization is sufficient to distinguish thick $Al_xGa_{1-x}As$ layers or large groups of thinner (3 nm or less) layers, individual or wide spaced small layers, particularly those with low Al content, are difficult to distinguish. Therefore, contrast was increased using a selective etchant.

Due to its availability, selectivity, and ease of use, a wet etchant combination of citric acid and hydrogen peroxide ($C_6H_8O_7/H_2O_2$) was chosen. $C_6H_8O_7/H_2O_2$ is a reaction-rate-limited etchant working by an oxidation−reduction mechanism, with the H_2O_2 acting as the oxidizing agent and the citric acid dissolving the resulting oxidized material. $C_6H_8O_7/H_2O_2$ can be used for a number of III−V material combinations.[10−14] Etch selectivity, defined as the ratio of etch rates, depends on the composition and doping of a sample, and can be vastly modified by changing the ratio of chemicals used. For $Al_xGa_{1-x}As$/GaAs samples etched with $C_6H_8O_7/H_2O_2$, etch rates decrease as x increases.[11] Due to the varying $Al_xGa_{1-x}As$ composition throughout the sample, it was important that etchant was selective between GaAs and $Al_xGa_{1-x}As$ with low Al content x. Previously reported etch selectivities for GaAs/$Al_{0.3}Ga_{0.7}As$ are generally in the 100:1 region (95,[10] 155,[11] 116[12]).

EXPERIMENTAL DETAILS

Sample Growth. $Al_xGa_{1-x}As$/GaAs superlattices were grown on a (100)-orientated Si-doped GaAs substrate by a VG VH80 molecular-beam epitaxy system. The sample consists of 3 sets of 5 superlattices, each of 10−14 layers. The first set consists of AlAs/GaAs layers of varying thickness but constant periodicity of 15.5 nm. The AlAs layer thickness ranges from 1 to 8.5 nm. The second set of superlattices has a constant AlAs layer thickness of 3 nm, and GaAs layers varying from 2 to 17 nm. The final set of superlattices has constant $Al_xGa_{1-x}As$/GaAs thickness (3 and 12.5 nm respectively), but different $Al_xGa_{1-x}As$ compositions x, ranging from 0.2 to 1.0. Each superlattice is separated by a 38−48 nm GaAs spacer, while each set of superlattices is separated by a 220−228 nm GaAs spacer.

Beam-Exit Cross-Sectional Polishing. Samples were mounted on a BEXP angled holder (5° slope) with an overhang of ∼300 μm. The beam entry surface was then filed down normal to the beam direction with 30, 9, and 1 μm diamond paper. The holder was placed within the vacuum chamber and BEXP was initiated at a vacuum of 2.0×10^{-5} mbar. Ion guns were allowed to warm up at a voltage of 3 kV for 10 min prior to processing at 6 kV. Once beam-exit occurred (approximately 2 h), voltage was decreased to 1 kV for 20 min to polish the surface. The process resulted in a cut of approximately 11° through the area of interest (with respect to the sample surface). Samples were subsequently cleaned in an ultrasonic bath using trichloroethylene, acetone, and isopropanol for 10 min each.

Etching. Several different $C_6H_8O_7/H_2O_2$ ratios and etch times were tested, with a 4:1 ratio etch for 30 s found to provide the required amount of contrast across the whole structure without removing too much material. Citric acid ($C_6H_8O_7$) was first produced by dissolving anhydrous citric acid crystals in deionized (DI) water with a ratio of 1 g of $C_6H_8O_7$ per 1 mL of DI H_2O. This solution was mixed with fresh 27% hydrogen peroxide (H_2O_2) at a 4:1 ratio. The $C_6H_8O_7/H_2O_2$ mixture was allowed to return to room temperature before etching. Samples were submerged in the etchant for 30 s without stirring. Samples were then rinsed in DI water for at least 1 min to stop the etching process.

Scanning Probe Microscopy. A Digital Instruments Multimode scanning prope microscope with a Nanoscope IIIa controller was used in an ambient environment. SPM was operated in tapping mode to provide an assessment using a basic and commonly available technique. Phosphorus (n) doped Si tips with a resonant frequency of approximately 300 kHz and force constant of approximately 50 N m^{-1} were used. Images were taken with fast scan direction perpendicular to the sample structure, and with a typical scan rate of 1−2 Hz. Images were analyzed using WSxM software.[15] Measurements for thin layers were made on 750 nm images produced at 512 samples/line. Thicker layers required larger scan sizes.

Transmission Electron Microscopy. A TEM analysis of the structure was undertaken in order to provide a comparison with the SPM data. A Jeol 2000FX transmission electron microscope operated

at 200 kV was used to study the sample, calibrated using a III−V superlattice structure with a period measured by double-crystal X-ray diffraction to an accuracy of better than 0.1%.

RESULTS AND DISCUSSION

Figure 2 shows composite BEXP-SPM and TEM images of the complete structure. In both cases, brighter layers are $Al_xGa_{1-x}As$

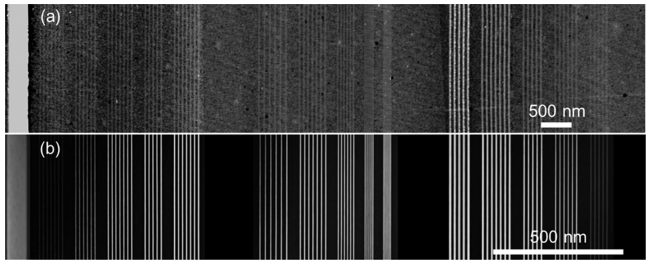

Figure 2. (a) Composite BEXP-SPM topography image combining three 5 μm scans of the complete structure etched with 4:1 $C_6H_8O_7/H_2O_2$ for 30 s. Vertical scale is 10 nm. The image has been desaturated for ease of comparison with TEM. (b) Composite TEM image of the same area. From left to right: 75 nm AlAs barrier layer, 3 nm $Al_xGa_{1-x}As$ composition x varying layers (0.2−1), 3 nm AlAs layers with different GaAs spacing, and differing thickness AlAs and GaAs layers (from 8.5 to 1 nm). Images have been resized to provide a comparative figure. Contrast and level have been modified slightly to increase clarity of layers in both images. The scale bars are different lengths due to the larger surface area scanned in a BEXP cross section.

while darker layers are GaAs. For BEXP-SPM, $Al_xGa_{1-x}As$ layers appear brighter than the surrounding GaAs due to a combination of oxide growth and the $C_6H_8O_7/H_2O_2$ etching GaAs much more rapidly than $Al_xGa_{1-x}As$. Although contrast is not as high as for TEM, all layers are clearly visible in the BEXP-SPM sample, with AlAs layers as thin as 1 nm being clearly distinguishable on the far right-hand side of the image. Contrast for both BEXP-SPM and TEM can be seen to increase with Al content x (left-hand side) and layer thickness (right-hand side). The center region of the structure consists of layers with constant Al composition and thickness, so contrast does not change.

Due to the unique sample geometry produced in the BEXP process (Figure 3), layer thicknesses can be measured by using the vertical movement of the cantilever between two points. Accuracy in these measurements is not solely dependent on the z-axis movement of the probe as the tip moves both vertically and laterally between points and as such care must be taken when determining the layer transition positions. However, the primary reliance on z-axis movement, combined with the larger lateral area scanned due to BEXP geometry, helps to reduce the tip-size effect on measurements. A number of scan profiles illustrating the variation in topography of the surface are presented in Figure 4. Measurements were made with zeroth-order flattened scans, with layer transition positions being determined by comparison with plane-fitted versions. Results were then compared with the TEM data for the structure.

Figure 5 shows the difference between SPM and TEM layer thickness measurements plotted against TEM layer thickness. A total of 167 layers were analyzed, the majority below 20 nm in thickness. The mean result of three measurements at different positions was used to determine the thickness of each layer. For thin layers, SPM measurements were found to be very close to the TEM values. Results are remarkably consistent, regardless

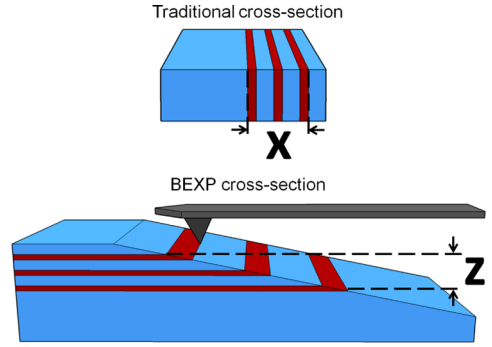

Figure 3. Comparison of traditional and BEXP cross sections. In a traditional cross section, image acquisition and measurements are undertaken in the direction illustrated using the lateral (x) motion of the tip. In a BEXP cross section, mounting the sample is much easier and the shallow cut angle means that each layer covers a much larger area, allowing easier identification using SPM techniques. The images obtained using this technique are therefore laterally at a larger scale than in a traditional cross section. The sample geometry means that layer thicknesses are determined by the vertical movement of the cantilever between two lateral points.

of layer composition, with the mean difference for layers under 20 nm thickness being just 0.1 ± 0.2 nm, or 2 ± 4% when expressed as percentage accuracy. For thicker layers, absolute accuracy decreases, although percentage accuracy correspondingly increases, with layers between 30 and 80 nm having a difference of 1 ± 2%. However, only a very limited number of measurements have been made for layers above 20 nm in size, so further work is required to determine accuracy for thicker layer measurements. It is expected that the precision of these measurements could be improved by integrating thickness measurements across the entire scan, rather than taking the mean result of a few measurements. However, we believe that the current method would be suitable for general measurements.

While TEM remains a more accurate method for the cross-sectional imaging of semiconductor nanostructures, the BEXP-SPM technique is an inexpensive and fast procedure. Furthermore, BEXP is not a particularly difficult technique to master and analysis requires just a basic familiarity with SPM methods. As such, we believe that BEXP-SPM is an excellent low-cost method for cross-sectional imaging of semiconductor samples containing quantum wells and superlattices. With further development, it should also be possible to image lower-dimensional structures such as quantum dots: such work is presently in progress. Given the huge variety of scanning probe techniques, BEXP also opens up the prospect of studying a range of magnetic, electronic, thermal, and optical properties of embedded nanostructures in cross section.

CONCLUSIONS

Beam-exit cross-sectional polishing (BEXP) produces a cross section through semiconductor samples with roughness on the nanoscale, making it suitable for qualitative and quantitative analysis of nanostructures with scanning probe microscopy (SPM). We successfully combined this technique with a light citric-acid/hydrogen-peroxide etch to image $Al_xGa_{1-x}As$/GaAs superlattice layers with thicknesses as low as 1 nm using tapping mode atomic force microscopy (AFM). SPM measurements were compared with transmission electron microscopy (TEM) analysis of the sample. The difference between layer

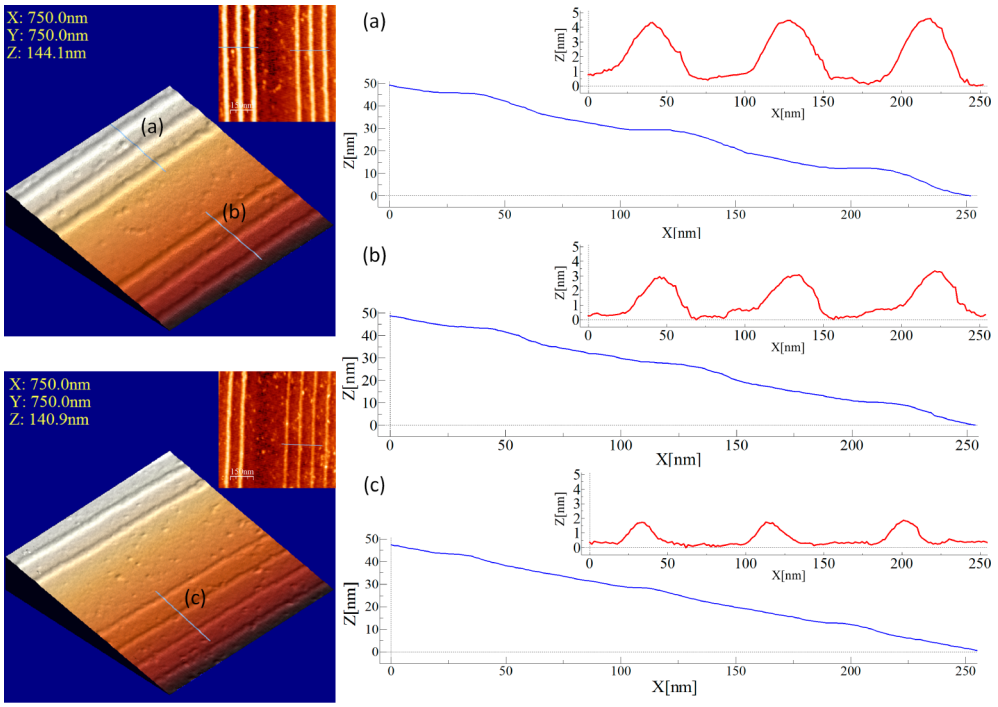

Figure 4. Examples of etched topographical scans (left), plane-fitted versions (inset) and scan profiles (right) used for layer thickness measurements. Actual topography is shown in blue while plane-fitted versions of the raw unfiltered data are shown in red. AlAs layer thicknesses are approximately (a) 8.5 nm, (b) 6.5 nm, and (c) 5 nm. As can be clearly seen, contour height due to the oxidation of AlAs layers reduces as layer thickness decreases. Vertical scale on the inset plane-fitted images is 5 nm.

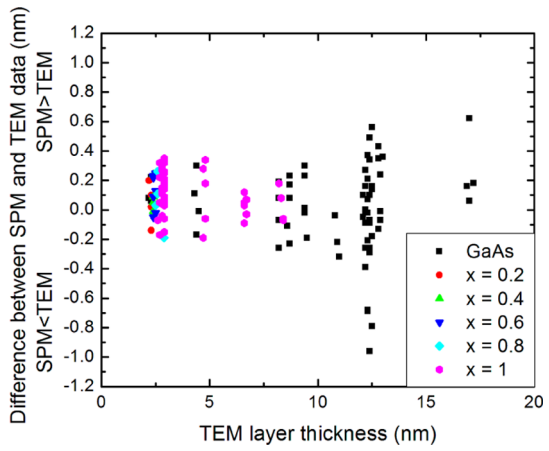

Figure 5. Comparison of TEM and SPM data for layers under 20 nm. Measurements for layer thicknesses are remarkably consistent, with the mean difference being just 0.1 ± 0.2 nm.

thicknesses measured by SPM and TEM was shown to be 0.1 ± 0.2 nm. BEXP-SPM thus shows great promise for the analysis of semiconductor heterostructures, especially devices with multiple layers such as vertical cavity surface emitting lasers, quantum cascade lasers and optical modulators.

AUTHOR INFORMATION

Corresponding Author

*Telephone: +44 1524 594750. E-mail: a.robson@lancaster.ac.uk.

Notes

The authors declare no competing financial interest.

ACKNOWLEDGMENTS

The authors would like to thank EPSRC for the award of a studentship for A.J.R. R.J.Y. gratefully acknowledges support from the Royal Society. This work was supported in part by the U.K. Engineering and Physical Sciences Research Council (EPSRC) including Grants EP/H006419 – QD2D Project, EP/G015570/1, EP/G06556X/1 (EPSRC-NSF), and the European Commission Award GRENADA (246073). A.M.S. thanks the Science City Research Alliance, AWM, ERDF, "Advanced Materials 1", and the HEFCE Strategic Development Fund for funding support.

REFERENCES

(1) Kolosov, O. V.; Grishin, I.; Jones, R. *Nanotechnology* **2011**, *22*, 185702.
(2) Kolosov, O. V.; Grishin, I. Patent WO/2011/101613, 25 August 2011.
(3) Jetté-Charbonneau, S.; Lahoud, N.; Charbonneau, R.; Mattiussi, G.; Berini, P. *IEEE Trans. Adv. Packag.* **2008**, *31*, 479–483.
(4) Rubanov, S.; Munroe, P. R. *Micron* **2004**, *35*, 549–556.
(5) Mogilevsky, P. *Ultramicroscopy* **2002**, *92*, 159–164.
(6) Takahashi, H.; Sato, A.; Takakura, M.; Mori, N.; Boerder, J.; Knoll, W.; Critchell, J. *Microchim. Acta* **2006**, *155*, 295–300.
(7) Amirmajdi, O. M.; Ashyer-Soltani, R.; Clode, M. P.; Mannan, S. H.; Wang, Y.; Cabruja, E.; Pellegrini, G. *IEEE Trans. Electron. Packag. Manuf.* **2009**, *32*, 265–271.
(8) Leica Microsystems webpage. http://www.leica-microsystems.com/fileadmin/downloads/Leica%20EM%20TIC020/Brochures/Leica_%20EM%20TIC020_brochure_en.pdf (accessed March 14, 2013).
(9) Reinhardt, F.; Dwir, B.; Kapon, E. *Appl. Phys. Lett.* **1996**, *68*, 3168–3170.
(10) Juang, C.; Kuhn, K. J.; Darling, R. B. *J. Vac. Sci. Technol., B: Microelectron. Process. Phenom.* **1990**, *8*, 1122–1124.

(11) Tong, M.; Ballegeer, D. G.; Ketterson, A.; Roan, E. J.; Cheung, K. Y.; Adesida, I. *J. Electron. Mater.* **1992**, *21*, 9−15.
(12) DeSalvo, G. C.; Tseng, W. F.; Comas, J. *J. Electrochem. Soc.* **1992**, *139*, 831−835.
(13) DeSalvo, G. C.; Kaspi, R.; Bozada, C. A. *J. Electrochem. Soc.* **1994**, *141*, 3526−3531.
(14) Tong, M.; Nummila, K.; Ketterson, A. A.; Adesida, I.; Aina, L.; Mattingly, M. *J. Electrochem. Soc.* **1992**, *139*, L91−L93.
(15) Horcas, I.; Fernandez, R.; Gomez-Rodriguez, J. M.; Colchero, J.; Gomez-Herrero, J.; Baro, A. M. *Rev. Sci. Instrum.* **2007**, *78*, 013705.